

Study of a Fragmentation Reaction by Thin-Target Recoil Techniques; Production of Na^{24} from Bismuth by 2.9-GeV Protons*

J. B. CUMMING, R. J. CROSS, JR.,† J. HUDIS, AND A. M. POSKANZER

Chemistry Department, Brookhaven National Laboratory, Upton, New York

(Received 4 November 1963)

The angular distribution of Na^{24} nuclei produced by bombardment of thin bismuth targets with 2.9-GeV protons has been measured. The forward-to-backward ratio in the laboratory system was found to be 1.52 ± 0.06 . Differential range curves for the Na^{24} nuclei have been obtained at angles of 15, 90, and 165°, with respect to the beam direction. The mean energy of emission at 90° is 47 MeV with a full width at half-maximum of 40 MeV. The mean is only 60% of the energy expected from Coulomb repulsion. Velocity spectra at 15 and 165° are nearly identical to the 90° spectrum linearly shifted by $\approx 10\%$ to higher and lower velocities, respectively. From the analysis of the angular distribution and the range data, we conclude that there is no moving system in which both the angular distribution and velocity spectra of the Na^{24} nuclei are symmetric about the direction perpendicular to the beam. This indicates that this typical fragmentation product is produced by a direct (rapid) process and not by the usual fast nucleonic cascade followed by a slower de-excitation step.

INTRODUCTION

THE concept of fragmentation to be discussed in this paper is that developed by Wolfgang *et al.*¹ In a study of the interaction with lead of protons having energies up to 3 GeV, these authors observed that products in the mass region 18 to 32 exhibit characteristic excitation functions which rise steeply from 0.4 to 2 GeV and then tend to level off at higher proton energies. Since these excitation functions appear to be characteristic of high deposition energies, and since meson production is known also to become increasingly probable above 0.4 GeV, Wolfgang *et al.*¹ postulated that meson production, scattering, and reabsorption during the intranuclear nucleon cascade lead to the creation of "hot spots" and to the breaking of many nucleon-nucleon bonds in some limited volume of the nucleus. The observed product or its progenitor would then issue from this highly excited region. The time scale for such a "fragmentation" process would be comparable to the transit times of energetic nucleons through the nucleus, and true thermal equilibrium over the whole nucleus would not be reached at the time of the breakup. A major contribution to the kinetic energies of the fragmentation products would be the Coulombic repulsion between the fragment and its partner. However, large distortions would probably exist at the moment of separation and the small fragment may capture some of the cascade nucleons. These effects would modify the energy from that of spheres in contact.

Excitation functions for forming F^{18} and Na^{24} from a wide variety of targets bombarded with 1- to 6-GeV protons were measured by Caretto *et al.*² For a given proton energy, the cross section for forming Na^{24} or

F^{18} decreases with increasing target mass number in the sequence Al, Cu, and Ag. However, for the heavier targets Ta, Au, Pb, and U, the probability of forming Na^{24} or F^{18} increases with increasing target mass number. These observations were interpreted as indicating that the mechanism for forming F^{18} or Na^{24} is different for the two branches of the cross section versus mass number curve. Yields from the light targets could be accounted for on the basis of a spallation-type mechanism, with the exception of silver at energies less than 2 GeV. From Ta, Au, Pb, and U targets, fragmentation, as defined by Wolfgang *et al.*,¹ was thought to be the dominant process. From the fact that Na^{24} production is ~ 5 times more probable than F^{18} production from Au, Pb, and U, it was postulated that these observed light nuclei are residues after evaporation from more neutron-excess primary fragments. Perfilov, Lozhkin, and Shamov³ have summarized a large amount of experimental data, including that obtained with nuclear emulsions, for the production of fragments and have considered various mechanisms for the fragmentation process.

Recently, Crespo, Alexander, and Hyde⁴ have used thick-target recoil techniques to investigate momentum transfer in the production of Na^{24} and Mg^{28} from Cu, Ag, Au, and U targets bombarded with energetic protons and alpha particles. They also reported cross sections for forming these products by 320- to 880-MeV alpha particles and by 700-MeV protons. From the analysis of the recoil data the mean kinetic energy of the Na^{24} or Mg^{28} was found to lie between 0.5 and 1.0 times that calculated from Coulomb repulsion between the Na^{24} or Mg^{28} and its complementary fragment. They interpreted this as indicating that, even in the case of copper, these light mass

* Research performed under the auspices of the U. S. Atomic Energy Commission.

† Present address: Harvard University, Cambridge, Massachusetts.

¹ R. Wolfgang, E. W. Baker, A. A. Caretto, J. B. Cumming, G. Friedlander, and J. Hudis, *Phys. Rev.* **103**, 394 (1956).

² A. A. Caretto, J. Hudis, and G. Friedlander, *Phys. Rev.* **110**, 1130 (1958).

³ N. A. Perfilov, O. V. Lozhkin, and V. P. Shamov, *Usp. Fiz. Nauk* **60**, 3 (1960) [English transl.: *Soviet Phys.—Usp.* **3**, 1 (1960)].

⁴ V. P. Crespo, J. M. Alexander, and E. K. Hyde, *Phys. Rev.* **131**, 1765 (1963); and V. P. Crespo, University of California Radiation Laboratory Report UCRL-9683, 1961 (unpublished).

products arise from division of the target into two fragments having a combined mass near that of the target. The recoil data also give values of the mean momentum transferred to the struck nucleus which rise linearly with the target mass number. If, independent of target mass, a monotonic increase of deposition energy with momentum transfer is assumed, then it follows that higher deposition energies are required for Na^{24} production from the higher mass targets than from the lower mass targets. Crespo *et al.*⁴ pointed out that such an increase contradicted the results of their analysis of the excitation functions in which the deposition energy was found to be independent of the target. Since the assumption of a two-step process was necessary for the analysis of the recoil data, they concluded that the contradiction was due to a breakdown of the two-step model; i.e., Na^{24} was not produced in a two-step process. However, it is not known whether the assumption of a monotonic increase of momentum transfer with deposition energy, independent of target mass, applies to Na^{24} production which, particularly at energies below 1 GeV, is a highly atypical process.

The aim of the present experiment was to investigate a typical fragmentation reaction: Na^{24} production from bismuth by 2.9-GeV protons. Thin-target recoil techniques were used to obtain angular distributions and differential energy spectra of the product nuclei. Interpretation of the results of such experiments is less ambiguous than those of thick-target studies, since it is not necessary to assume relationships between momentum transfer and excitation. As will be shown, we conclude that fragmentation occurs at a time when memory of the nucleonic cascade has not been lost, and hence this process does lie outside of the framework of a two-step mechanism.

ANGULAR DISTRIBUTION MEASUREMENTS

The angular distribution of Na^{24} nuclei produced by irradiating thin bismuth targets with 2.9-GeV protons in the Brookhaven Cosmotron was measured. The apparatus and the irradiation techniques used were basically the same as have been previously described.⁵ The targets were $\frac{1}{2}$ -in. squares of vacuum deposited bismuth supported on 0.00025-in.-thick Mylar foils. The catcher foils were three layers of 0.004-in. or 0.003-in. Mylar for the angles less than or greater than 90° from the beam direction, respectively. As will be seen below, one such foil is sufficiently thick to stop essentially all Na^{24} recoils. The second layer of Mylar was used to measure the blank arising from activation of impurities in the foil by scattered radiations. This blank was always less than 5% of the activity of the first foil. In a given experiment a range of angles from $7\frac{1}{2}^\circ$ to $97\frac{1}{2}^\circ$ to the beam direction was subtended by the catchers. The target foil was perpendicular to the $52\frac{1}{2}^\circ$ direction so

that the Na^{24} nuclei which were collected had paths in the target inclined at $\leq 45^\circ$ to the normal. To obtain the angular distribution in the backwards direction the entire apparatus was reversed.

After irradiation with an integrated circulating beam of from 1×10^{14} to 4×10^{14} protons (not counting multiple traversals through the target foil), the assembly was taken apart and the catchers cut into 15° sections. These were separately dissolved in trifluoroacetic acid containing 5 mg of Na carrier as sodium acetate. From the solutions, sodium was purified by standard radiochemical procedures. The final mounting form was NaCl, and the Na^{24} activity of each sample was assayed with end-window flow-type beta proportional counters. For the relatively low counting rates in the blank samples, anticoincidence shielding was used to reduce backgrounds. The various counters were intercalibrated with Na^{24} or Cl^{36} standards. Chemical yields were generally high (60–70%) and reproducible in a given irradiation. Experiments showed that the variation of counting efficiency with sample thickness could be neglected for the range of thicknesses encountered in this study.

Angular distributions were obtained for two target thicknesses, 0.24 mg/cm² bismuth (“thin”) and 0.72 mg/cm² (“standard”). The results are presented in Table I. For each target thickness, the results from separate irradiations in the forward and backward directions have been joined by overlap at the 90° point and the entire curves normalized so that

$$\int_0^\pi 2\pi I(\theta) \sin\theta d\theta = 4\pi. \quad (1)$$

The standard deviations of the values in Table I have been compounded from the errors due to counting statistics, cutting of the foils ($\pm 1\%$), chemical yields

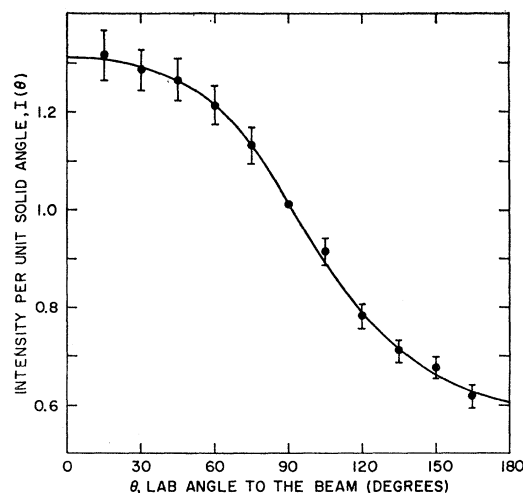


FIG. 1. Angular distribution in the laboratory system of Na^{24} recoils from an 0.24-mg/cm² bismuth target.

⁵ A. M. Poskanzer, J. B. Cumming, and R. Wolfgang, Phys. Rev. **129**, 374 (1963).

TABLE I. Angular distribution in the laboratory system of Na²⁴ nuclei produced by the interaction of 2.9-GeV protons with bismuth.

Angle, ^a θ (degrees)	Intensity per unit solid angle, $I(\theta)$	
	0.72-mg/cm ² target	0.24-mg/cm ² target
15	1.208±0.038	1.316±0.051
30	1.255±0.038	1.286±0.042
45	1.227±0.037	1.265±0.042
60	1.183±0.036	1.214±0.039
75	1.091±0.033	1.132±0.037
90	1.003 ^b	1.012 ^b
105	0.919±0.028	0.915±0.028
120	0.849±0.026	0.782±0.025
135	0.813±0.025	0.711±0.023
150	0.691±0.021	0.677±0.022
165	0.649±0.021	0.618±0.023
F/B ^c	1.38 ±0.08	1.49 ±0.09
η_θ ^c	0.15 ₉ ±0.02 ₇	0.19 ₇ ±0.02 ₈

^a Angle with respect to the beam direction of the center of each catcher foil. Angular resolution was ±7½° from the central angle.
^b Intensities from the forward and backwards hemispheres have been normalized at the 90° points.
^c See text for definition of F , B , and η_θ .

(±1.5%), counter efficiency variations (±1%), and the blank correction (±50% of the absolute value of the blank). The 0.24-mg/cm² data are plotted in Fig. 1. These data have not been corrected for the 15-deg angular resolution since the correction for this effect is very small (≤0.3%).

The data of Table I indicate an increased forward peaking of the angular distribution (but within the sum of the errors) for the thin target compared to the thicker one. This is in the direction that would be expected if there were some scattering of the recoils by the target and its backing. Also included in Table I are the forward to backward intensity ratios, F/B , for each target. Here F is the integrated intensity (in fraction of the total) in the forward hemisphere and B is the integrated intensity in the backward one. The quantity⁶ η_θ in Table I is defined as

$$\eta_\theta = F - B \tag{2}$$

and will be of interest in the later analysis of the results. An independent value of η_θ was obtained from a separate experiment in which the Na²⁴ recoils from an 0.29-mg/cm² bismuth target supported on an 0.19-mg/cm² Formvar film were collected with catchers in a 2 π geometry. Of the total Na²⁴ produced, 3.7% was retained by the target plus backing. It was estimated from the range data, which will be presented later, that 2% of this was in the Formvar (which was in the forward direction from the bismuth) and 1.7% in the bismuth itself. From this experiment η_θ was found to be 0.210±0.023. The mean η_θ from the thin-target angular distribution and the 2 π experiment is 0.20₅±0.01₈ and the corrected F/B ratio is 1.51₆±0.05₇.

⁶ The quantity η_θ as defined here is approximately the commonly used "thin target" η , see L. Winsberg, Report UCRL-8618, p. 44, 1958 (unpublished).

RANGE-CURVE MEASUREMENTS

Differential range curves for Na²⁴ recoiling from ≈0.71-mg/cm² bismuth targets were obtained at angles of 15, 90, and 165° to the beam direction. The targetting arrangements for these measurements are shown in Fig. 2. Catcher foils were 0.00025-in. (≈0.9 mg/cm²) Mylar and they subtended angular intervals of 15° centered on the desired angles. The geometry of the catchers was such that ≈25% of the total number of recoils in the desired angular interval were collected on the foils. After irradiation, the Na²⁴ activity of each foil was obtained as described above. Data obtained for the range curves are presented in Table II. These results have been corrected for the blank due to activation of impurities as measured by foils beyond the Na²⁴ range. In each case, one-half the thickness of the target in units of equivalent stopping power of Mylar has been added to the ranges. To further interpret these results a range-energy curve is needed. We have extrapolated the ranges of O¹⁶, F¹⁹, and Ne²⁰ ions in aluminum as meas-

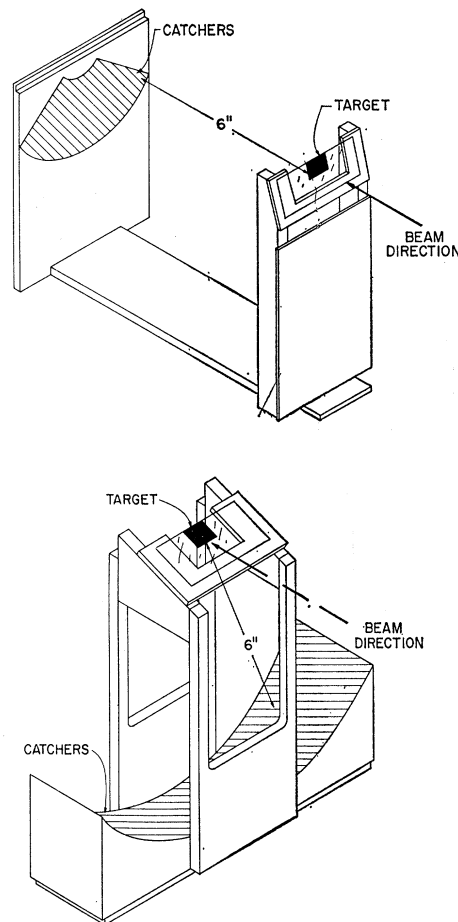


FIG. 2. Target arrangements for measuring differential range curves at 15° (top) and 90° (bottom) to the beam direction. The 165° range curve was obtained by reversing the apparatus used for the 15° measurement.

TABLE II. Differential range curves for Na²⁴ produced by the interaction of 2.9-GeV protons with bismuth.

Range interval (mg/cm ²)	Angle with respect to the beam direction				
	15°	90°	90°	165°	
	Intensity ^a	Range interval (mg/cm ²)	Intensity ^a	Range interval (mg/cm ²)	Intensity ^a
0.14- 1.13	19.5±1.3	0.14- 1.08	141.7± 2.8	0.15-1.13	61.5±1.7
1.13- 2.12	32.9±1.7	1.08- 2.02	207.0± 4.4	1.13-2.11	134.4±2.9
2.12- 3.09	98.8±2.4	2.02- 2.95	461.6± 9.4	2.11-3.09	304.2±5.7
3.09- 4.10	195.4±4.0	2.95- 3.89	822.1±15.7	3.09-4.07	336.3±6.5
4.10- 5.09	252.7±4.9	3.89- 4.83	866.6±16.6	4.07-5.05	204.0±3.8
5.09- 6.08	234.2±4.8	4.83- 5.77	656.2±13.1	5.05-6.03	101.4±2.3
6.08- 7.07	167.6±4.3	5.77- 6.70	364.2± 6.8	6.03-7.01	34.2±1.2
7.07- 8.07	105.9±2.4	6.70- 7.64	176.9± 3.5	7.01-7.99	12.1±0.5
8.07- 9.06	57.6±1.7	7.64- 8.58	89.9± 1.8	7.99-8.97	4.4±0.3
9.06-10.05	31.3±2.9	8.58- 9.52	44.5± 1.0	8.97-9.95	2.4±0.8
10.05-11.03	18.4±1.8	9.52-10.46	24.2± 1.2		
11.03-12.02	9.6±1.1	10.46-11.39	11.3± 0.5		
12.02-13.01	6.4±1.1	11.39-12.33	5.1± 0.3		

^a Intensity is in arbitrary units. However, in each experiment it is approximately the Na²⁴ counting rate (counts/min) at the start of counting.

ured by Northcliffe⁷ to obtain a range curve for Na²⁴ in aluminum. In the low-energy region, the data of Poskanzer⁸ were also used. The range curve for Na²⁴ in Mylar was obtained from that in aluminum by multiplying the range at any energy by 0.783, the factor experimentally determined by Schambra *et al.*⁹

The energy spectrum of Na²⁴ nuclei recoiling at 90° to the beam is shown in Fig. 3. The energy spectrum is peaked with a full width at half-maximum of ≈40 MeV. The mean energy is 47 MeV, in agreement with the value interpolated between the 46- and 57-MeV mean energies obtained by Crespo *et al.*⁴ for Na²⁴ emission from Au and U targets, respectively. The mean energy is only 60% of that expected from the Coulomb repul-

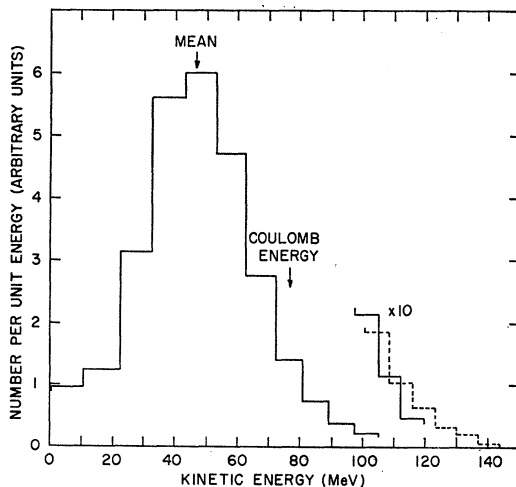


FIG. 3. Kinetic energy spectrum of the Na²⁴ recoils emitted at 90° to the beam direction from an 0.71-mg/cm² bismuth target. The broken curve was obtained from a 2-mg/cm² target and was normalized to the solid curve near the peak.

⁷ L. C. Northcliffe, Phys. Rev. **120**, 1744 (1960).

⁸ A. M. Poskanzer, Phys. Rev. **129**, 385 (1963).

⁹ P. E. Schambra, A. M. Rauth, and L. C. Northcliffe, Phys. Rev. **120**, 1758 (1960).

sion between two spheres, Na²⁴ and Ho¹⁷¹, in contact.¹⁰ However, the high-energy tail of the distribution extends to ≈140 MeV. It is clear that there are relatively few low-energy (<20 MeV) Na²⁴ recoils which suggests that Na²⁴ is emitted from or has a massive partner. The normalized intensity in this low-energy region observed with a 2 mg/cm² target was nearly double that shown in Fig. 3. We feel that this indicates that most, if not all, of the low-energy Na²⁴ recoils arise from scattering in the target and its backing. Such an effect is consistent with the apparent variation of the angular distribution with target thickness.

Range straggling is not a significant contributor to the width of the observed energy spectrum. Bohr¹¹ has pointed out that for heavy ions, the major contribution to straggling occurs in the nuclear stopping region near the end of the range. Poskanzer⁸ has reported a half-width of 0.20±0.05 mg/cm² independent of energy for 1.0-, 2.0-, and 2.8-MeV Ne²² ions stopping in aluminum. Hence, the uncertainty in range due to straggling is considerably less than one foil and can be ignored.

ANALYSIS OF DATA AND DISCUSSION

We will now examine the experimental results to see what conclusions can be drawn about the mechanism of Na²⁴ production from bismuth. We will adopt the formalism of the two-step model, analyze the data as if this model applied, and then show that contradictions result. It is assumed that the laboratory velocity v_L of a particular recoil can be represented as the sum of two vectors,

$$v_L = v + V. \quad (3)$$

Here v is the velocity imparted to the struck nucleus by

¹⁰ For this calculation, ⁷⁸Pt¹⁹⁵ was taken as the fissioning nucleus and a radius parameter $r_0 = 1.44$ F was used.

¹¹ N. Bohr, Kgl. Danske Videnskab. Selskab, Mat. Fys. Medd. **18**, No. 8 (1948).

the nucleonic cascade¹² and \mathbf{V} is the velocity imparted to the Na^{24} by the subsequent breakup of the struck nucleus. In a system moving with the velocity \mathbf{v} , the angular distribution of \mathbf{V} should be symmetric about 90° to the beam direction, provided that memory (except for angular momentum) of the first step has been lost. In a moving system the angular distributions for various values of \mathbf{V} will not necessarily all be the same. As a consequence, the velocity spectrum of recoils in the moving system need not be independent of angle, but must be the same at a given angle and at its supplement. In general there will be distributions of \mathbf{v} and possibly correlations between \mathbf{v} and \mathbf{V} as well. These must be considered in the detailed analysis of the data.

To analyze the range curves, we transform them to the velocity distributions plotted in Fig. 4. These distributions are very nearly Gaussian except in the low-velocity region. (The dashed curves in Fig. 4 show Gaussians through the 15 and 165° data.) The fraction of events in the low-velocity tails varies from 1.5% for the 15° curve to 5% for the 165° curve. As has been pointed out above, these amounts increase with target thickness and are believed to arise from scattering in the target and its backing. The Gaussian shapes of the distributions have been used to eliminate the low-velocity tails and to correct for the finite resolution of each foil before calculating average velocities in the three directions. These means and the standard deviations of the distributions are given in Table III. Because of the small variation of velocity with angle, the effects of the 15-deg angular resolution are small and may be ignored. The major contribution to the errors of the mean values comes from possible nonuniformities in the thickness of the catcher foils. Based on weights of a number of foils, we estimate $\pm 2\%$ as a conservative limit for this effect. An additional 165° range curve was obtained with the target reversed accidentally. When analyzed as above and corrected for the foil supporting the target, the mean velocity from this experiment was found to be 1.80 ± 0.04 $(\text{MeV}/\text{amu})^{1/2}$, in excellent agreement with the value in Table III. The widths of the distributions at the three angles are not very different and the trend observed may not be outside experimental errors. With the assumption that the spectrum of \mathbf{V} is independent of angle, the absence of significant broadening of the 90° distribution compared to the 15 and 165° curves and the absence of a shift of the 90° mean from the average of the 15 and 165° means indicates that any component of \mathbf{v} perpendicular to the beam direction has a very small effect on our results.¹² However, it cannot be ruled out that these observations arise from

¹² We have assumed for simplicity that \mathbf{v} is along the beam direction. The effect of a component of \mathbf{v} perpendicular to the beam (v_\perp) on the angular distribution is discussed in Ref. 5. For the differential range measurements, a perpendicular component of \mathbf{v} would broaden the 90° velocity distribution and also shift its mean to a higher velocity by a factor of approximately $[1 + \frac{1}{2}(v_\perp/V)^2]$.

TABLE III. Mean velocities and standard deviations of the velocity distributions as a function of angle to the beam direction.

Angle (degrees)	Mean velocity $(\text{MeV}/\text{amu})^{1/2}$	Standard deviation $(\text{MeV}/\text{amu})^{1/2}$
15	2.17 ± 0.04	0.39
90	1.98 ± 0.04	0.37
165	1.78 ± 0.04	0.33

accidental cancellation of the effects of v_\perp and the variation of the spectrum of \mathbf{V} .

We will now obtain values of $\langle v \rangle$ and $\langle V \rangle$ from the mean velocities, $\langle v_L \rangle_{15}$ and $\langle v_L \rangle_{165}$, given in Table III. The analysis would have been particularly simple if the experiments had been performed at angles of 0 and 180° . In that case,

$$\langle v \rangle = \frac{1}{2} (\langle v_L \rangle_0 - \langle v_L \rangle_{180}) \quad (4)$$

and

$$\langle V \rangle = \frac{1}{2} (\langle v_L \rangle_0 + \langle v_L \rangle_{180}). \quad (5)$$

Relatively small corrections ($\leq 3.5\%$) are necessary to these equations, however, to make them applicable to the data at 15 and 165° . In this manner we obtain values of $\langle v \rangle = 0.202 \pm 0.028$ $(\text{MeV}/\text{amu})^{1/2}$ and $\langle V \rangle = 1.975 \pm 0.028$ $(\text{MeV}/\text{amu})^{1/2}$ from the 15 and 165° mean velocities. The 90° mean yields an independent value of $\langle V \rangle = 1.985 \pm 0.040$ $(\text{MeV}/\text{amu})^{1/2}$. (The 90° mean is very nearly equal to $\langle V \rangle$ since the forward effect of v is minimal.) From these values we calculate a

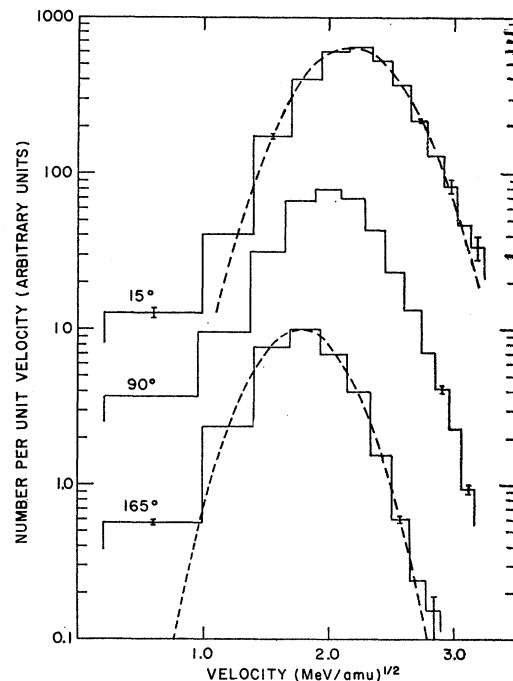


FIG. 4. Velocity spectra of the Na^{24} recoils at 15, 90, and 165° to the beam direction in the laboratory system from a 0.71-mg/cm² bismuth target. The curves are arbitrarily displaced vertically for display purposes. The broken curves are Gaussian fits to the data excluding the low-velocity regions.

value of

$$\eta_R \equiv \langle v \rangle / \langle V \rangle = 0.10_2 \pm 0.02_0. \quad (6)$$

The error on this value includes an estimate of the effect of uncertainty in the slope of the range-velocity relationship. (In the region of interest, range is nearly proportional to energy.)

It can be shown⁶ that η_θ as defined by Eq. (2) is equal to $\langle v/V \rangle$, provided the assumption of a two-step mechanism is valid. In the absence of correlations between v and V ,

$$\eta_\theta = \langle v/V \rangle = \langle v \rangle \langle 1/V \rangle = \eta_R \langle V \rangle \langle 1/V \rangle. \quad (7)$$

The term, $\langle V \rangle \langle 1/V \rangle$ is evaluated to be 1.04_7 from the 90° velocity spectrum, hence η_θ determined from the angular distribution measurements should be only $\approx 5\%$ larger than η_R . The observed difference by a factor of two is significant and may be taken as indicating a breakdown of the two-step model. (There is a preferred emission of Na^{24} in the forward direction compared to the prediction of a two-step model.)

This conclusion, however, depends on the absence of a correlation between v and V . Preliminary calculations had indicated that a strong negative correlation could account for the value of η_θ being substantially greater than η_R . Such correlations can be ruled out by the following considerations of the shapes of the velocity spectra. For this purpose the 15 and 165° velocity spectra shown in Fig. 4 have been extrapolated to 0 and 180° , respectively, and their intensities, $I(0^\circ)$ and $I(180^\circ)$ have been normalized to agree with those of the angular distribution in Fig. 1. (The small extrapolations greatly simplify the following calculations.) The data are then in the form of double differential cross sections, $\partial^2 N / \partial v_L \partial \Omega$. From Eq. (3) for the 0° and 180° spectra,

$$\langle v_L \rangle_0 = V + v = V + f(V) \quad (8)$$

and

$$\langle v_L \rangle_{180} = V - v = V - f(V). \quad (9)$$

In (8) and (9), v has been replaced by $f(V)$ to indicate the possible correlation. We have chosen as convenient for calculational purposes, a functional form

$$v = \langle v \rangle + k(V - \langle V \rangle). \quad (10)$$

Here the sign of k determines the direction of the correlation and the magnitude of k its strength. The 0° and 180° velocity spectra have been transformed from distributions of v_L into distributions of V for several values of k . The transformation function is given by

$$\left(\frac{\partial^2 N}{\partial V \partial \Omega'} \right) = \left(\frac{\partial^2 N}{\partial v_L \partial \Omega} \right) \left(\frac{V}{v_L} \right)^2 \frac{dv_L}{dV}. \quad (11)$$

For each of the transformed distributions, the standard deviation, σ , and intensity (area), $I = dN/d\Omega'$, have been calculated and are presented in Table IV as a function of k . The values of these quantities in the laboratory system are included for comparison.

TABLE IV. Dependence of the standard deviations and intensities of the velocity distributions as a function of the correlation between v and V .

Assumed correlation	Standard deviation of the velocity distribution (MeV/amu) ^{1/2}		Intensity ratio $I(0^\circ)/I(180^\circ)$
	$\sigma(0^\circ)$	$\sigma(180^\circ)$	
$k = -0.4$	0.58	0.25	1.30
$k = 0$	0.37	0.33 ₅	1.40 ± 0.14
$k = 0.05$	0.36	0.35	1.41
$k = 0.1$	0.34 ₅	0.37	1.43 ± 0.14
$k = 0.4$	0.28	0.51 ₅	1.50
Lab system	0.39	0.33	2.15 ± 0.11

If Na^{24} is produced by a two-step mechanism, it should be possible to have $\sigma(0^\circ) = \sigma(180^\circ)$ and $I(0^\circ)/I(180^\circ) = 1.0$ simultaneously. Examination of Table IV indicates that this is not possible and that our previous conclusion of forward peaking is not in error due to correlations of v and V . Other functional forms of the correlation could be considered. Any sufficiently strong negative correlation could be expected to result in an intensity ratio of unity, but with significantly different widths of the forward and backward distributions in the transformed system. This is quantitatively shown by the entry in Table IV for $k = -0.4$. We feel that our conclusion that Na^{24} is not produced by a two-step mechanism is more general than the specific correlation function [Eq. (10)] which has been used to demonstrate it.

It is interesting to note that the value of $k \approx 0.05$, for which $\sigma(0^\circ) = \sigma(180^\circ)$, lies between the values of k for two simple cases and is probably indistinguishable, within errors, from them. When $k = 0$, v is a constant, or in a more general sense there is no correlation between v and V . The case, $k = 0.10_2 = \eta_R$, corresponds to a constant value of the ratio $\langle v/V \rangle$.

We have now shown that the combination of angular distribution and velocity spectra measurements has ruled out a two-step model for Na^{24} production from bismuth at 3 GeV. However, the velocity spectra are suggestive of a modified two-step process in which memory of the beam direction has not been lost at the time of the second step. The laboratory angular distribution (Fig. 1) has been transformed¹³ into one such system by using $\eta = k = 0.10_2$. The resulting distribution¹⁴ is shown in Fig. 5. This shows preferential emission of Na^{24} in the forward hemisphere with an $F/B = 1.20 \pm 0.08$. Once a two-step process has been ruled out there is no longer a unique intermediate system. The system above has been chosen because of its simplicity and to approximately symmetrize the means and stand-

¹³ Convenient tables for this transformation as a function of η and angle have been tabulated by J. B. Marion, T. I. Arnette, and H. C. Owens, Oak Ridge National Laboratory Report ORNL 2574, 1959 (unpublished).

¹⁴ If an analytical form for the transformed angular distribution is desired, $a + b \cos^2 \theta + c \cos \theta$ is suitable. The data shown in Fig. 5 are well fit by this functional form with $b/a = -0.11_4$ and $c/a = 0.16_4$.

ard deviations of the velocity distributions. However one could choose an intermediate system in which the mean velocity forward is greater than that backward. The limiting case in this direction is the laboratory system. Such angular distributions would indicate that there is an even greater preference for the Na^{24} fragments to originate in the forward hemisphere of the nucleus. The transformation necessary to obtain an $F/B=1$ in the absence of correlations would require a value of $\eta_\theta=0.20_6\pm 0.01_8$. In such a system the Na^{24} nuclei emitted in the backward direction would have higher mean velocity than those emitted in the forward direction, which seems unlikely. In the presence of correlations equal mean velocities could probably be achieved, but, as is shown in Table IV, at the expense of a very much narrower velocity distribution in the backward direction. This also seems unlikely.

Additional Discussion

Dostrovsky, Fraenkel, and Hudis¹⁵ have calculated from evaporation theory the cross sections for He^6 , Li^8 , Be^7 , and N^{13} production from heavy element targets and have obtained reasonable agreement with the experimental values. Such a model would give rise to a Na^{24} energy spectrum qualitatively like that observed since the Coulomb barrier suppresses the emission of low-energy particles. If the energy spectrum of Fig. 3 is replotted in the form $\ln[I(\epsilon)/\epsilon]$ versus ϵ , an apparent nuclear temperature of ≈ 11 MeV is obtained from the portion of the curve above 70 MeV, where it is nearly linear. This analysis assumed a unique excitation energy, which appears doubtful in this case. It serves primarily to indicate a very high temperature, comparable to the mean binding energy (≈ 8 MeV) of nucleons in a heavy nucleus such as bismuth. The lifetime of such a system based on the estimate of Ericson,¹⁶ would be comparable to the transit times of relativistic particles across the nuclear diameter. Equipartition of energy certainly cannot occur in such short times and application of the statistical model as used by Dostrovsky *et al.*¹⁵ to explain N^{13} production does not appear justified in the case of Na^{24} production from bismuth. Rather than to suppose the existence of excitation energies comparable to total binding energies, it may be assumed that the observed temperature is characteristic of some limited hot region of the nucleus from which the Na^{24} originates, which is to say again that Na^{24} production is a prompt process occurring before equipartition.

If the fragmentation of bismuth is a rapid process, it is unreasonable to expect any substantial change in the neutron to proton ratio of the fragment from that of the target nucleus (for bismuth, $N/P=1.518$), and the most probable primary fragments thus should have a greater neutron excess than Na^{24} . The primary frag-

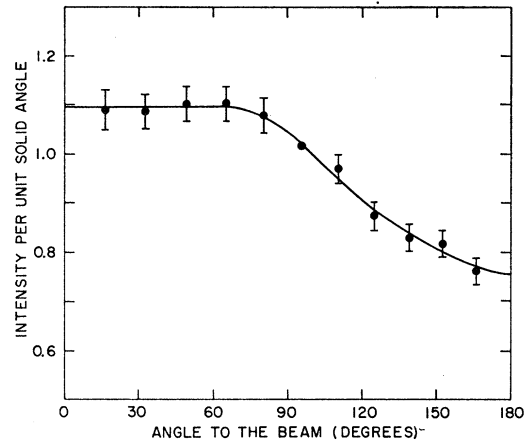


Fig. 5. Angular distribution of the Na^{24} recoils in a moving system chosen to symmetrize the velocity distributions.

ments should also be excited because of the distortions of shape at the moment of division and because some of the cascade particles may be captured by them. These conclusions were also drawn by Wolfgang *et al.*¹ The observed products presumably arise from the primary ones by evaporation of some nucleons, or, if the excitation energy is low enough, by beta decay. Evaporation of nucleons will tend to reduce the energy of the Na^{24} recoils from that of the primary fragment because of the reduction in mass. However, if the primary fragments have charges greater than 11, this effect would, at least in part, be compensated for by higher primary fragment energies resulting from the increased Coulomb repulsion. The opposite effect will be observed for those Na^{24} formed by beta decay from less highly charged progenitors. That such a large fraction of the Na^{24} recoils have energies below that predicted from Coulomb repulsion is rather surprising and is a problem that any detailed theory of fragmentation must explain. It may indicate very substantial distortions from spherical shape at the moment of division.

CONCLUSIONS

The production of Na^{24} , a typical fragmentation product, from bismuth by 2.9-GeV protons cannot be explained by a two-step mechanism in which the second step has no memory of the first. This follows from the contradiction, if such a model is assumed, between the results of angular distribution and range measurements. This conclusion is independent of any assumptions of the relation between momentum transfer and excitation energy which were critical to the analysis of Crespo *et al.*⁴ Although the present experiment does not measure the time scale for fragmentation, some limits can be set. A lower limit, the time for the development of the prompt cascade (nuclear diameter/velocity of light), is $\approx 6 \times 10^{-23}$ sec. It is reasonable to expect angular momentum to be transferred to the nucleus by the

¹⁵ I. Dostrovsky, Z. Fraenkel, and J. Hudis, Phys. Rev. **123**, 1452 (1961).

¹⁶ T. Ericson, Advan. Phys. **9**, 495 (1960).

cascade. However, if the excited nucleus rotates, any preferential location of "hot spots," say in the forward hemisphere, will be lost before decay. For a value of $J=10$, the time to rotate 180° is $\approx 3 \times 10^{-20}$ sec and this is then the order of an upper limit for the fragmentation process.

We feel that the mechanism for fragmentation proposed by Wolfgang *et al.* is basically in agreement with the present observations. Fragmentation occurs during or shortly after the development of the nuclear cascade and before equipartition of energy is established. The fragments arise from regions of the nucleus which are highly disturbed ("hot spots"). The present experiment indicates that these excited regions are more concentrated in the forward hemisphere of the nucleus. The energies of most of the fragments are less than Coulombic, which may indicate large deviations from spherical shape at the moment of fragment formation.

We agree with Crespo *et al.*⁴ that meson production, scattering, and reabsorption are not *necessary* for fragmentation and that Wolfgang *et al.*¹ may have overemphasized their role. Meson production, scattering and reabsorption in proton induced cascades will certainly increase the probability for the creation of highly disturbed regions and subsequent fragmentation. So also may bombardment with the correlated nucleons in an alpha particle as was observed by Crespo *et al.*

ACKNOWLEDGMENTS

The authors wish to thank Miss E. Norton for performing the chemical yield analyses and R. Withnell for target preparation. We are indebted to Dr. J. Alexander, Dr. G. Friedlander, Dr. J. R. Grover, Dr. S. Katcoff, Dr. M. L. Perlman, Dr. N. Sugarman, and Dr. A. Turkevich for many interesting discussions of our results and conclusions.

Pseudoscalar Charge Density of Spin- $\frac{1}{2}$ Particles. I. Existence*

K. HIDA†

Argonne National Laboratory, Argonne, Illinois

(Received 4 November 1963)

When interactions are renormalizable and are invariant under time reversal but not invariant under space reflection, then under the requirement that the S matrix is free from divergences after renormalization it is shown that any spin- $\frac{1}{2}$ particle with nonvanishing mass should have pseudoscalar charge density in addition to the usual scalar charge density. Unrenormalizable interactions are also discussed as possible sources of the pseudoscalar charge density. Arguments are given for the observability of the pseudoscalar charge density.

1. INTRODUCTION AND DERIVATION OF THE PSEUDOSCALAR CHARGE DENSITY

THE purpose of this work is to study the electromagnetic properties spin- $\frac{1}{2}$ particles possess as a result of parity-nonconserving but time-reversal invariant interactions. The purpose of this section is to show that any charged spin- $\frac{1}{2}$ particle has pseudoscalar charge density in addition to usual scalar charge density as a result of the parity-nonconserving interactions. To show this, let us consider the Lagrangian density

$$L = L_1 + L_2, \quad L_1 = - : \bar{\psi}(x) \left[\gamma_\mu \frac{\partial}{\partial x_\mu} + m_0 \right] \psi(x) : \quad (1.1)$$

for a spin- $\frac{1}{2}$ field ψ in the Heisenberg representation, where the notation $:X:$ means to take the normal product of the operators included in X , ψ^* is the Hermitian conjugate of ψ , $\bar{\psi} = \psi^* \beta$, and γ_μ is a 4×4

Hermitian matrix and satisfies the commutation relation

$$\{\gamma_\mu, \gamma_\nu\} = 2\delta_{\mu\nu}. \quad (1.2)$$

The interaction Lagrangian density L_2 is always assumed to be invariant under time reversal. To prove unambiguously that the pseudoscalar charge density exists, L_2 is assumed (for the moment) to include only renormalizable interactions.

The next step is to renormalize the wave function ψ for the free dressed particle with moment p interacting with its self-field as

$$\psi(p) = Z_2^{1/2} \psi_I(p), \quad (1.3)$$

where ψ_I represents the wave function in interaction representation and the c number Z_2 is a positive definite constant. Since the term $\bar{\psi} \gamma_\mu \gamma_5 (\partial/\partial x_\mu) \psi$ is invariant under time reversal but the term $\bar{\psi} \gamma_5 \psi$ is not, the former term as well as the self-energy term $\bar{\psi} \psi$ should be induced by the self-interaction of any spin- $\frac{1}{2}$ particle with finite mass, where $\gamma_5^2 = 1$. To renormalize as (1.3) shows, therefore, both the parity-nonconserving counter

* Work performed under the auspices of the U. S. Atomic Energy Commission.

† On leave of absence from the Research Institute for Fundamental Physics, Kyoto University, Kyoto, Japan.